

Optical density of states in ultradilute GaAsN alloy: Coexistence of free excitons and impurity band of localized and delocalized states

Sumi Bhuyan, Sanat K. Das, Sunanda Dhar, Bipul Pal, and Bhavtosh Bansal

Citation: *Journal of Applied Physics* **116**, 023103 (2014); doi: 10.1063/1.4886178

View online: <http://dx.doi.org/10.1063/1.4886178>

View Table of Contents: <http://scitation.aip.org/content/aip/journal/jap/116/2?ver=pdfcov>

Published by the [AIP Publishing](#)

Articles you may be interested in

[Photoluminescence properties and high resolution x-ray diffraction investigation of BInGaAs/GaAs grown by the metalorganic vapour phase epitaxy method](#)

J. Appl. Phys. **112**, 063109 (2012); 10.1063/1.4752031

[Near band-edge luminescence and evidence of the weakening of the N-conduction-band coupling for partially relaxed and high nitrogen composition GaAs_{1-x}N_x epilayers](#)

J. Appl. Phys. **102**, 073716 (2007); 10.1063/1.2786675

[Thickness dependence of exciton and polariton spectra from ZnSe films grown on GaAs substrates](#)

J. Appl. Phys. **90**, 6114 (2001); 10.1063/1.1415061

[Growth and optical characterization of indirect-gap Al_xGa_{1-x}As alloys](#)

J. Appl. Phys. **86**, 418 (1999); 10.1063/1.370746

[Photoluminescence and photoreflectance studies of defects in GaAs epitaxial layers grown by liquid phase epitaxy at different supercooling temperatures](#)

J. Vac. Sci. Technol. A **15**, 971 (1997); 10.1116/1.580950



AIP | Journal of Applied Physics

Journal of Applied Physics is pleased to announce **André Anders** as its new Editor-in-Chief

Optical density of states in ultradilute GaAsN alloy: Coexistence of free excitons and impurity band of localized and delocalized states

Sumi Bhuyan,¹ Sanat K. Das,² Sunanda Dhar,² Bipul Pal,¹ and Bhavtosh Bansal^{1,a)}

¹Indian Institute of Science Education and Research Kolkata, Mohanpur Campus, Nadia 741252, West Bengal, India

²Department of Electronic Science, University of Calcutta, 92 A.P.C. Road, Kolkata 700009, India

(Received 6 May 2014; accepted 19 June 2014; published online 9 July 2014)

Optically active states in liquid phase epitaxy-grown ultra-dilute GaAsN are studied. The feature-rich low temperature photoluminescence spectrum has contributions from excitonic band states of the GaAsN alloy, and two types of defect states—localized and extended. The degree of delocalization for extended states both within the conduction and defect bands, characterized by the electron temperature, is found to be similar. The degree of localization in the defect band is analyzed by the strength of the phonon replicas. Stronger emission from these localized states is attributed to their giant oscillator strength. © 2014 AIP Publishing LLC.

[<http://dx.doi.org/10.1063/1.4886178>]

Since the discovery of giant bandgap bowing in GaAs_{1-x}N_x ($x \leq 5\%$), these pseudo-binary alloys have been actively studied.¹⁻⁵ GaAs_{1-x}N_x belongs to a class of mismatched semiconductor alloys (other examples include InSb_{1-x}As_x, ZnTe_{1-x}Se_x),⁶ where the virtual crystal approximation, so successful in modeling the alloys like Ga_{1-x}Al_xAs or Ga_{1-x}In_xP, breaks down. A number of unusual properties are observed in GaAs_{1-x}N_x alloys. For example, contrary to the prediction of $\mathbf{k} \cdot \mathbf{p}$ theory, the electron effective mass increases even as the energy gap is reduced on alloying.⁷ Furthermore, due to the relatively large difference in size and electronegativity between the anion elements, GaAs_{1-x}N_x is thought to have a miscibility gap in the growth phase diagram.⁸ This leads to its tendency to phase-separate and form clusters. The optical and electronic properties are often dominated by the electronic states associated with these localized cluster states.^{9,10} The localized states manifest in an order of magnitude larger alloy disorder scattering potential compared to other semiconductor alloys, leading to degradation of carrier mobility, large Urbach tail in the absorption edge,¹¹ “S-shape” in the temperature dependence of the peak emission energy,¹² and large Stokes’ shift between absorption and emission.¹³

An isolated nitrogen dopant forms a resonant level with the conduction band states and, on account of alloying, these conduction band states are highly perturbed as the nitrogen concentration is increased.^{1-5,10} After 15 years of intensive study, the recent interest in GaAs_{1-x}N_x has shifted to focusing on N concentrations less than 0.5% for understanding how the band structure evolves as one goes from the very heavy doping (parts per hundred thousand) to the dilute alloy (parts per hundred) limit.¹⁴⁻¹⁹

This paper discusses the nature of light emitting states in ultra-dilute GaAs_{1-x}N_x observed through a very complex emission spectrum. We will present strong evidence for the existence of both localized and delocalized states within the continuum of states forming the defect band,¹⁸⁻²⁰ address

the controversy whether the low energy peaks in the emission spectra are phonon-assisted transitions or from a separate set of cluster states,²¹⁻²³ and finally discuss the quantum mechanical enhancement of the excitonic oscillator strength on account of the localization of its center of mass.²⁴

GaAs-GaN alloys can normally only be grown under highly non-equilibrium conditions using molecular beam epitaxy, metal-organic vapor phase epitaxy, or forced incorporation of nitrogen into GaAs by ion bombardment, followed by annealing and possibly hydrogenation steps.²⁻⁴ In each case, the nitrogen atoms may be located at metastable positions and the electronic and optical properties may differ between samples and between different growth techniques.

We, on the other hand, have previously demonstrated that epitaxial GaAs_{1-x}N_x/GaAs can be grown by the liquid phase epitaxy (using GaAs + Ga + GaN melt with 2% molar Li₃N as a flux for nitrogen dissolution in GaAs) under close to equilibrium conditions.²⁵ The advantage of studying such melt-grown samples is that GaAs_{1-x}N_x is more likely to be in an equilibrium phase and the conclusions of the studies based on such samples may have more generic (sample-independent) validity. With such samples, one is of course limited to the ultra-dilute alloy limit. Photoluminescence (PL) measurements were conducted in a helium closed-cycle optical cryostat in the temperature range of 4–80 K. The sample was excited with a 643 nm diode laser and the spectra were dispersed with 500 mm spectrograph equipped with a charge-coupled device. The incident excitation power was varied over three orders of magnitude between 15 and 1500 μ W.

PL at 4 K at a low excitation power of 16 μ W is shown in Fig. 1. The peaks above 1.46 eV are attributed to usual free and bound exciton states from the GaAs substrate. In addition to these, we observe a distinct peak at 1.450 eV and a set of peaks below 1.408 eV. If the free-exciton transition arising from the hybridized conduction band due to alloying in GaAs_{1-x}N_x identified with the 1.450 eV peak, one infers $x \approx 0.25\%$.^{16,23} The structure in the transitions below 1.408 eV is attributed to phonon replicas. This is discussed in detail later.

^{a)}Electronic mail: bhavtosh@iiserkol.ac.in

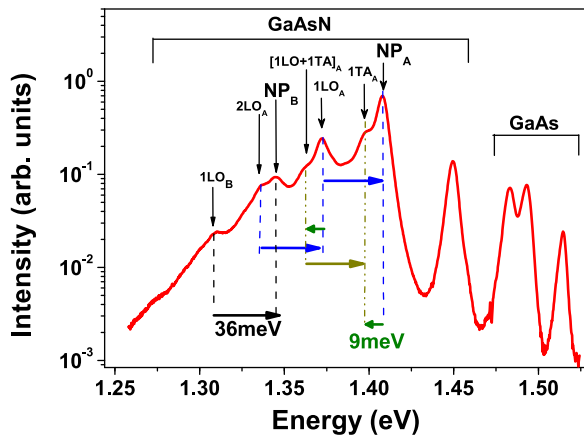


FIG. 1. PL at 4K with small excitation power $64 \mu\text{W}$. Emission beyond $\sim 1.475 \text{ eV}$ is attributed to the GaAs substrate. Emission at 1.45 eV is attributed to free excitons, and at and below 1.408 eV to cluster states. Many phonon replicas corresponding to first and second order (TA, LO, and TA + LO) transitions are also observed.

In Figs. 2 and 3, we have plotted the excitation power and temperature dependence of PL, respectively. To facilitate a direct comparison between the emission channels associated with various transitions, spectra are arbitrarily scaled so that the peak around 1.408 eV has nearly the same intensity in the particular figure. Consider the excitation power-dependent spectra (Fig. 2) first. Especially at the highest excitation power, the spectrum consists of broad continuous emission between 1.30 and 1.45 eV with a busy structure indicating the presence of many different types of excitonic states.

The peak at 1.450 eV , which is about a factor of 5 weaker than 1.408 eV peak at the lowest power, progressively gains strength, and, at the highest excitation power, exceeds the 1.408 eV peak by about a factor of 2. This implies that the density of states responsible for the emission from the peaks marked as NP_A and NP_B and its various satellites is much smaller than those responsible for the free exciton peak at 1.450 eV . This fact is also borne out in the temperature-dependent spectra (Fig. 3). The bound state

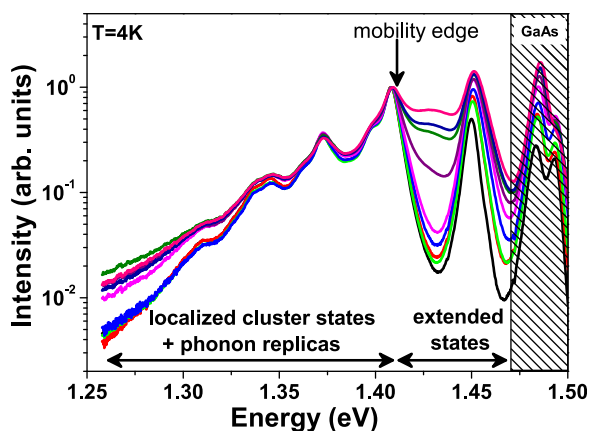


FIG. 2. PL spectra at 4K when the excitation power is varied between 0.1 mW and 11 mW . The spectra are scaled so that the intensity at $\sim 1.408 \text{ eV}$ is the same for all. The emission below 1.408 eV is attributed to localized cluster states and their phonon replica and above 1.408 eV to continuum states. A “mobility edge” separates the continuum states from localized states at 1.408 eV .

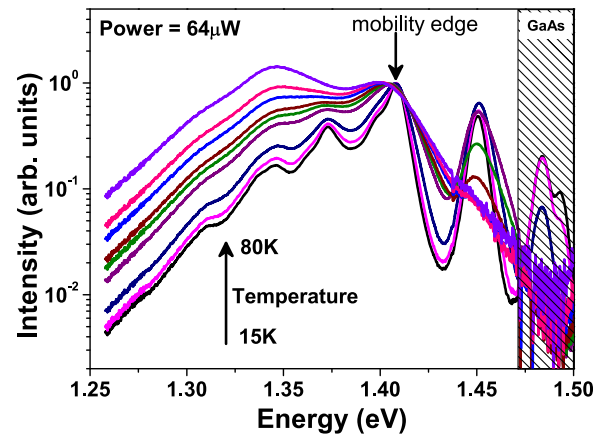


FIG. 3. Temperature dependence of the PL spectra between 15 and 80 K , measured at the excitation power of $64 \mu\text{W}$. The spectra are scaled so that the intensity at $\sim 1.40 \text{ eV}$ is the same for all. Note that exponential tails (straight lines on this semi-log graph) develop at the high energy sides of the peaks at 1.40 and 1.45 eV as the temperature is increased. The slight redshift is due to the usual decrease in the fundamental gap with temperature. The relative intensity of the phonon replicas becomes larger than the non-phonon peak at higher temperatures.

emission in comparison with the band states is clearly more robust against the increase in temperature, as it is for defect states in $\text{In}_x\text{Ga}_{1-x}\text{N}$ alloys and quantum dots.²⁶

Second, continuum emission between ~ 1.41 and 1.45 eV , which was missing in Fig. 1, becomes progressively prominent at high excitation powers (Fig. 2). For spectra measured at lower excitation powers (Fig. 3), these states are visible in the high energy tail at elevated temperatures. The exponential form of the tail implies that the carriers have a Maxwell-Boltzmann distribution with an effective “carrier temperature” T_e , inferred by fitting $PL \sim \exp[-(E - E_0)/k_B T_e]$ in this energy window (Fig. 4).^{27,28} Here, E_0 represents the relevant energy gap. The rationale behind this fit is that

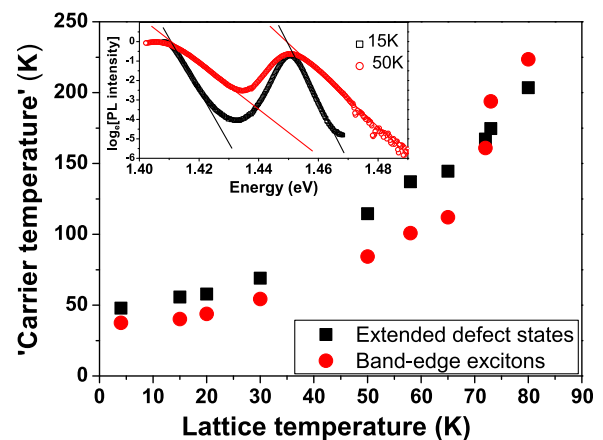


FIG. 4. (Inset) Prescription for determining the electron temperature: Natural logarithm of PL intensity plotted in the relevant range of energy and the high energy tails of the two peaks corresponding to the emission from delocalized states in the defect band ($\sim 1.40 \text{ eV}$) and the band-edge excitons are fitted to straight lines whose slope is used to infer the “carrier temperature,” T_e . This procedure for two temperatures (15 K and 50 K) is shown. (Main figure) Inferred carrier temperatures for the two bands are plotted as the function of lattice temperature. The fact that two T_e 's closely follow each other implies that electrons in both the bands are delocalized to a similar degree.³⁰

while the lower energy cut-off of the PL emission spectrum arises from the density of states, the high energy region (assuming that the band width is very large compared to $k_B T_e$) tail represents the carrier distribution function.²⁹ The occupation probability can thus be characterized by a single parameter, T_e . Fits for spectra measured at two representative temperatures (15 K and 50 K) are shown in Fig. 4 (inset).

It has been previously shown that not just the kinetic energy but also the extent of carrier localization can be characterized by T_e . If photoexcited carriers are created with equal probability anywhere within a band, once trapped they will end up recombining from higher energy states. From the above expression for PL, complete trapping would imply a uniform occupation probability within a band and thus an infinite carrier temperature.^{13,27,30} In Fig. 4, carriers from both the free excitonic states (~ 1.45 – 1.47 eV) and states between ~ 1.41 and 1.45 eV have nearly the same T_e . That T_e for both bands closely follows each other for a large range of lattice temperatures indicates that carriers in both these states are equally delocalized and experience similar disorder. Fig. 4 thus independently establishes the existence of two separate sets of extended states within two distinct bands.

The second band of extended states between ~ 1.41 and 1.45 eV are identified with states where the excitons percolate through the crystal by overlaps with their neighbors. It is also evident from Figs. 2 and 3 that the localized states within the defect band continuously (in energy) merge with the delocalized (supercluster)¹⁷ states. The value of energy where this transition occurs is marked with an arrow in Figs. 2 and 3. While this has previously been called the “mobility edge,” it is emphasized that this designation is not quite conventional. Historically, the “mobility edge” had been predicted to appear within a band as the result of a subtle wave interference phenomenon resulting solely on account of disorder (Anderson transition).²⁰ In principle, there should be two such mobility edges, appearing on both the high and the low energy band edges where the density of states is small. In the present case, however, the sharp boundary between the localized and the extended states within the defect band is more perhaps a percolation phenomenon. The classification of various states inferred from the above analysis is schematically depicted in Fig. 5.

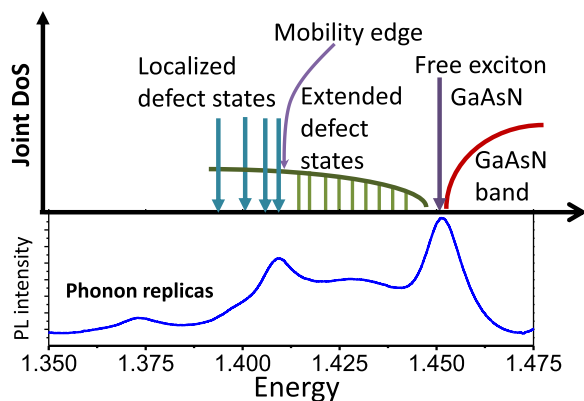


FIG. 5. Schematic of the joint density of states observed through optical transitions in $\text{GaAs}_{0.9975}\text{N}_{0.0025}$ along with the 4 K PL spectrum measured at high power.

Phonon replicas. Most of the low energy peaks below 1.41 eV can be identified with one of the two prominent transitions, labeled “ NP_A ” and “ NP_B ,” as they occur at a separation of the longitudinal-optical (LO) (36 meV)³¹ and/or the transverse-acoustic (TA) (9 meV)³¹ phonon modes from these two no-phonon lines (Fig. 1). While the correct energy separation alone is not sufficient to mark these transitions as phonon replicas,²¹ the combination of the observations in Figs. 2 and 3 give additional support to this assertion. In Fig. 2, intensity of the phonon replicas scales linearly with the strength of the no-phonon transitions, even though the excitation power is varied by almost three orders of magnitude. The relative intensities of the replicas between themselves and with respect to the no-phonon peaks are (almost) preserved. This is only likely to happen if it is the same set of states that are involved for emission at various energies. The relative intensities of other transitions in the broad continuum below ~ 1.35 eV, on the other hand, are found to be strongly power-dependent and non-monotonic. In Fig. 3, the phonon-assisted transitions broaden and gain in strength due to larger occupation probability of phonons at higher temperature.

The electron-phonon coupling is expected to enhance on account of localization in the cluster states. No replicas are observed for the extended excitonic states and above the mobility edge in the impurity band (Energy > 1.408 eV). The Huang-Rhys’ single frequency configuration coordinate model provides a standard method to analyze these phonon-assisted transitions within bound states.^{32,33} The strength of vibronic coupling resulting in n^{th} phonon-replica is parameterized by a temperature-dependent dimensionless number $S_n = n! I_n / I_0$ where I_0 and I_n are the strengths of the zero-phonon transition and its n^{th} phonon-replica. Following Stoneham,^{32,33} the calculation of the Huang-Rhys factor S can be done assuming Fröhlich coupling of polar-optical phonons with the localized electronic wave functions. Focussing on the first replica

$$S_1 = e^2 / \pi \hbar \omega_{\Gamma} (1/\epsilon_{\infty} - 1/\epsilon_0) \int_0^Q F(\mathbf{q}) d\mathbf{q}. \quad (1)$$

Here $F(\mathbf{q})$ is the overlap of the bound state wave functions with the phonon plane waves of momentum \mathbf{q} . Here the notation is standard and we have completely followed Ref. 32. Given that the estimated binding $E_B \approx 43$ meV, the bound states associated with nitrogen cannot be treated as simple hydrogenic levels and perhaps a better (though still arbitrary) choice of the wave function would be those corresponding to a delta-function potential, $\phi_0(r) = (\beta/2\pi)^{1/2} r^{-1} \exp[-\beta r]$, where the inverse localization length is simply estimated from the uncertainty argument, $\beta \approx \sqrt{2m^* E_B / \hbar^2}$.^{32,33} Since it is the electron which is bound to the isoelectronic nitrogen impurity, we take $m^* = 0.067$. This gives $\beta \approx [4.4 \text{ nm}]^{-1}$. $F(\mathbf{q}) = [\pi/2 - \arctan(2\beta/q)]^2 (2\beta/q)^2$,³² when plugged into Eq. (1) yields a relatively large (though still very much in the weak coupling regime) value of $S \approx 0.25$. Experimentally, $S_1 = I_1 / I_0$ for the NP_A transition has a value of $S_1 = 0.35$ and for NP_B , $S_1 = 0.25$ (Fig. 1). The agreement between experiment and theory is only expected to be approximate because of the very simple nature of the analysis that ignores the non-adiabatic nature of the interaction.

Giant oscillator strength. It was recognized in the late 1990s that disorder-created localized states may not always be a nuisance but may actually be responsible for relatively strong and thermally stable emission both in InGaN and quantum dots.²⁶ Note that there is expected to be an additional enhancement of the emission efficiency on account of the excitons being bound.^{24,34} Though this phenomenon has been known since 1962, it has received scant attention in the context of dilute nitrides.

As long as the size of the bound exciton is much smaller than the wavelength of light, coherence effects enhance the oscillator strength f_{bound} of the bound exciton compared to that of the free exciton f_{free} though the approximate relationship: $f_{bound}/f_{free} \approx 4\pi(1/\beta)^3/\Omega_0 \approx 133$. Here, $\Omega_0 = 0.18 \text{ nm}^3$ is the unit cell volume GaAs and $1/\beta \approx 4.4 \text{ nm}$ was already calculated earlier. Hence, these bound states have about two orders of magnitude higher radiative recombination efficiency compared to the free exciton states.

To summarize, this paper attempted an insight into the nature of the energy levels in the highly mismatched GaAs_{0.9975}N_{0.0025} alloy by studying an equilibrium-grown sample in the ultra-dilute limit. The zoo of observed optical transitions (Fig. 1) could be consistently explained on account of two separate bands below the GaAs conduction band associated with free excitons and defect states (Figs. 2 and 3). The defect states continuum itself has coexisting localized and extended states. The degree of delocalization for the latter is similar to that of hybridized conduction band states (Fig. 4). (Only) The bound states transitions below the “mobility edge” were found to have strong phonon replicas. We have also pointed out that these bound state transitions should have more than two orders of magnitude enhanced optical activity due to the giant oscillator strength effect of account of exciton localization. This is an additional reason for observation of strong emission from these localized levels up to much higher temperature.

ACKNOWLEDGMENTS

BP thanks DST and INSA, the Government of India for partial financial support.

¹W. Shan *et al.*, *Phys. Rev. Lett.* **82**, 1221 (1999).

²*Physics and Applications of Dilute Nitrides*, edited by I. A. Buyanova and W. M. Chen (Taylor & Francis, New York, 2004).

³*Dilute Nitride Semiconductors*, edited by M. Henini (Elsevier, Oxford, 2005).

⁴*Dilute III–V Nitride Semiconductors and Material Systems*, edited by A. Erol (Springer, Berlin, 2008).

⁵E. P. O’Reilly, A. Lindsay, P. J. Klar, A. Polimeni, and M. Capizzi, *Semicond. Sci. Technol.* **24**, 033001 (2009).

⁶A.-B. Chen and A. Sher, *Semiconductor Alloys* (Plenum, New York, 1995).

⁷F. Masia *et al.*, *Phys. Rev. B* **73**, 073201 (2006).

⁸S. B. Zhang and S.-H. Wei, *Phys. Rev. Lett.* **86**, 1789 (2001).

⁹R. Kudrawiec, M. Latkowska, M. Baranowski, J. Misiewicz, L. H. Li, and J. C. Harmand, *Phys. Rev. B* **88**, 125201 (2013).

¹⁰A. Lindsay and E. P. O’Reilly, *Phys. Rev. Lett.* **93**, 196402 (2004).

¹¹B. Bansal, V. K. Dixit, V. Venkataraman, and H. L. Bhat, *Appl. Phys. Lett.* **90**, 101905 (2007).

¹²T. Nuytten, M. Hayne, B. Bansal, H. Y. Liu, M. Hopkinson, and V. V. Moshchalkov, *Phys. Rev. B* **84**, 045302 (2011).

¹³B. Bansal, A. Kadir, A. Bhattacharya, B. M. Arora, and R. Bhat, *Appl. Phys. Lett.* **89**, 032110 (2006).

¹⁴A. Polimeni *et al.*, *Phys. Rev. B* **77**, 155213 (2008).

¹⁵K. Alberi, B. Fluegel, D. A. Beaton, A. J. Ptak, and A. Mascarenhas, *Phys. Rev. B* **86**, 041201(R) (2012).

¹⁶B. Fluegel, K. Alberi, D. A. Beaton, S. A. Crooker, A. J. Ptak, and A. Mascarenhas, *Phys. Rev. B* **86**, 205203 (2012).

¹⁷K. Alberi, S. A. Crooker, B. Fluegel, D. A. Beaton, A. J. Ptak, and A. Mascarenhas, *Phys. Rev. Lett.* **110**, 156405 (2013).

¹⁸Q. X. Zhao, S. M. Wang, Y. Q. Wei, M. Sadeghi, A. Larsson, and M. Willander, *Phys. Lett. A* **341**, 297 (2005).

¹⁹Y. Zhang, A. Mascarenhas, J. F. Geisz, H. P. Xin, and C. W. Tu, *Phys. Rev. B* **63**, 085205 (2001).

²⁰U. Jahn, M. Ramsteiner, R. Hey, H. T. Grahn, E. Runge, and R. Zimmermann, *Phys. Rev. B* **56**, R4387 (1997).

²¹K. Hantke *et al.*, *J. Mater. Sci.* **43**, 4344 (2008).

²²X. Liu, M. E. Pistol, L. Samuelson, S. Schwetlick, and W. Seifert, *Appl. Phys. Lett.* **56**, 1451 (1990).

²³P. J. Klar *et al.*, *Appl. Phys. Lett.* **76**, 3439 (2000).

²⁴C. H. Henry and K. Nassau, *Phys. Rev. B* **1**, 1628 (1970).

²⁵S. K. Das, T. D. Das, and S. Dhar, *Semicond. Sci. Technol.* **26**, 085028 (2011).

²⁶K. P. O’Donnell, R. W. Martin, and P. G. Middleton, *Phys. Rev. Lett.* **82**, 237 (1999).

²⁷M. Gurioli, A. Vinattieri, J. Martinez-Pastor, and M. Colocci, *Phys. Rev. B* **50**, 11817 (1994).

²⁸J. Szczytko, L. Kappei, J. Berney, F. Morier-Genoud, M. T. Portella-Oberli, and B. Deveaud, *Phys. Rev. Lett.* **93**, 137401 (2004).

²⁹R. Bhattacharya, B. Pal, and B. Bansal, *Appl. Phys. Lett.* **100**, 222103 (2012).

³⁰B. Bansal, *J. Appl. Phys.* **100**, 093107 (2006).

³¹J. L. T. Waugh and G. Dolling, *Phys. Rev.* **132**, 2410 (1963).

³²Y. Zhang, W. Ge, M. D. Sturge, J. Zheng, and B. Wu, *Phys. Rev. B* **47**, 6330 (1993).

³³A. M. Stoneham, *J. Phys. C: Solid State Phys.* **12**, 891 (1979).

³⁴I. Pelant and J. Valenta, *Luminescence Spectroscopy of Semiconductors* (Oxford University Press, Oxford, 2012).